Contribution adjacent modes for circular microstrip antenna loaded by two annular rings

Raed M. Shaaban **Zeki A. Ahmed** **Wa'il A. Godaymi**

Basra Unv./Sci.Col./Phys.Dep
mus.raad@yahoo.com

Abstract:

In this paper, theoretical study of circular microstrip antenna loaded by two annular rings (CMSAL2AR) and calculation the contribution of the adjacent modes and studied positively or negatively affected on the antenna's coefficients (Bandwidth and Directive Gain).The proposed antenna using principle equivalence with moment of method formulation of electromagnetic radiation to find unknown electric current density on the conductor surface , and both unknowns electric and magnetic density current on the dielectric surface which are responsible for the generation of far fields radiation in the space for the components (E_θ ,E_φ) . From the radiation pattern can be calculated with contribution of the adjacent mode. The directive gain increased to (G= 19.92 dB) and bandwidth has been better (BW%= 19.9%) when this contribution is affect positively at the ratioR_{ab}=5.5 and R_{ab}=6.5respectively.

http://dx.doi.org/10.31257/2018/JKP/100106

Keywords: CMSAL$_2$AR, Adjacent modes, Radiation pattern, Bandwidth, Directive gain.

مساهمة الأنماط المجاورة للنمط الرنيني لهوائي شريطي دائري محمل بحلقتين معدنية

رائد مسلم شعبان **زكي عبد الله احمد** **وائل عبد اللطيف كديمي**

جامعة االبصرة / كلية العلوم / قسم الفيزياء

الخلاصة:

يقدم البحث الحالي دراسة نظرية لتصميم هوائي شريطي دائلري محمل بحلقتين معدنيتين وحساب الأنماط المجاورة للنمط الرنيني وتأثيراتها الإيجابية والسلبية على معاملات الهوائي المختلفة مثل عرض الحزمة والتحصيل .استخدم في التحليل الرياضي للهوائي المقترح طريقة العزوم مع مبدأ التكافؤ لحل المسئلة الكهرومغناطيسية للاشعاع وحساب معاملات التيار الكهربائية والمغناطيسية المكافئة على السطوح المختلفة للهوائي قيد الدراسة ، والتي من خلالها تم حساب المركبات المستعرضة للمجالات الكهرومغناطيسية لتحديد معاملات الهوائي المختلفة تحت تاثير تداخل الأنماط.

من اهم النتائج التي حصلنا عليها إثر التأثير الإيجابي للانماط المجاورة لهذا الهوائي كانت عند النسبة (R_{ab}=5.5) حيث كانت الزيادة واضحة في عرض الحزمة (19.9%) وفي التحصيل (19.92 dB).

الكلمات المفتاحية: الهوائي قيد الدراسة، الأنماط المجاورة، الهيكل الاشعاعي، عرض الحزمة، التحصيل الاتجاهي.

1. Introduction

In recent years, the microstrip antenna is one of the most important type's antennas that took a great interest in both theoretical, experimental researches and engineering applications due to lightweight, small size and ease manufacturing. A microstrip antenna geometry consists of three main parts in its simplest case. The first part is a radiating patch, which is usually made from a good conductor materials printed on one side of a dielectric substrate, which is the second part. The third part is a ground plane, which is also made from a good conductor printed on the other side of the dielectric substrate, [1, 2].Also the microstrip possess a very narrow frequency bandwidth and low efficiency also .There are many methods that significantly reducing the effect of the problem mentioned above , and many researches have devoted their studies to improve these coefficients. A number of theoretical and experimental researches have been done to improve the bandwidth of the antenna [3]. Loading of shorting pins and stacking of patches are some techniques to increase the bandwidth of microstrip antennas [4]. Different shapes of slot loading in fed patch also enhance the antenna bandwidth [5].In this paper, using loaded to the patches as in proposed antenna (circular microstrip antenna loaded two annular ring) is used.

2. Antenna Design

The antenna under test is designed as a circular microstrip antenna loaded by annular rings conductor. The dimensions of these rings were chosen for improving the antenna parameter as the band width, and directive gain as shown in Figure (1).This Fig shows a different dimension for the loading radiated region of the antenna and the dielectric spaces. This dimension can be substituted by certain percentages to include all the important components parts of the antenna which were used to calculate the radiation fields and all the parameters of this antenna .The value (R_{ab}) represents the ratio between loaded patch region radius (b) and the circular disk radius (a). This ratio has great influence in improving the antenna coefficients because it represents the controlling of the region of electromagnetic coupling between the external and internal rings with the circular disc .The value $(ab = ab_1 + ab_2)$ which is the sum of the two rings width, and (h_{123}) which is the total dielectric layer region between the conductor part of the patch (h_2, h_3) is added this to the outer substrate (h_1) , are important parameters that effect positive or negative on the result .

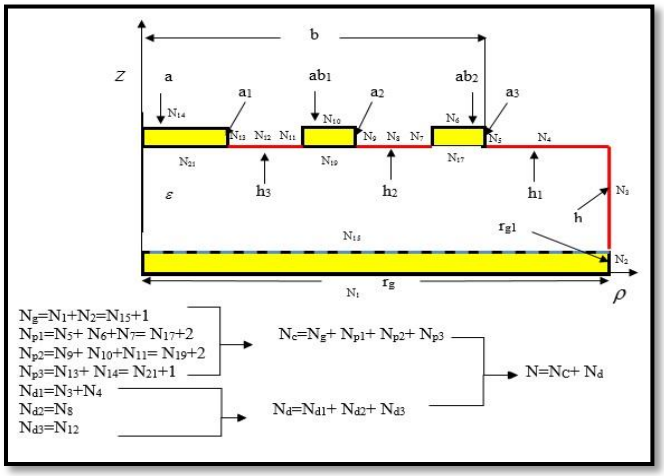

Figure (1) Proposed antenna design.

3. Mathematical Analysis

The theoretical studies to solving the electromagnetic problem issues previously is based on Method of Moment is used here to solve the electromagnetic problem of the field components is distributed on the surfaces of aCMSAL2AR.

The high calculations ability of this method in solving the integral equation, since it included all the boundary conditions of the current densities on different surface and the easiest in suggesting the test functions as the conjugate of the basis function, according to Galerkin's model. This made it as the most important numerical techniques in addition to the help of the body of revolution principle and the application of equivalence principle. Now we will represent the electric and magnetic fields in these calculated the volume V by the electric and magnetic equivalent surface cur-

rents, these currents are defined as [6] :

$\vec{J}_s = \hat{n} \times \vec{H}_s$, onS … (1a)

$\vec{M}_s = -\hat{n} \times \vec{E}_s$, onS … (1b)

Where $\vec{J}_S, \vec{M}_S$ represent electric and magnetic surface currents densities respectively.

According to the equivalence, principle will be divided as two regions. These regions are a finite region of volume $V^e$and a finite region of volume V^d as shown in figures (2) and (3).

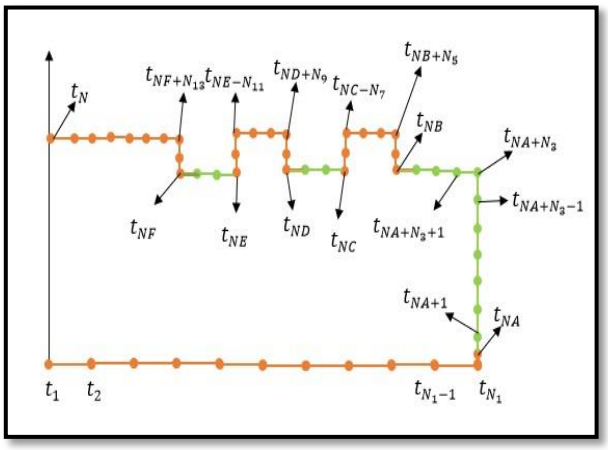

Figure (2): Equivalent for region V^e.

Table (1): The distribution of basis function for external equivalence region.

Basis function number	Location	Symbol	Equivalent symbol
$N_1 + N_2$	Ground plan	N_g	$N_A \equiv N_g$
$N_3 + N_4$	Dielectric(N_{d1})	N_{d1}	$N_B \equiv N_A + N_{d1}$
$N_5 + N_6 + N_7$	External annular ring	N_{p1}	$N_C \equiv N_B + N_{p1}$
N_8	Dielectric (N_{d2})	N_{d2}	$N_D \equiv N_C + N_{d2}$
$N_9 + N_{10} + N_{11}$	Internal annular ring	N_{p2}	$N_E \equiv N_D + N_{p2}$
N_{12}	Dielectric (N_{d3})	N_{d3}	$N_F \equiv N_E + N_{d3}$
$N_{13} + N_{14}$	Circular patch	N_{p3}	$N_N \equiv N_F + N_{p3}$

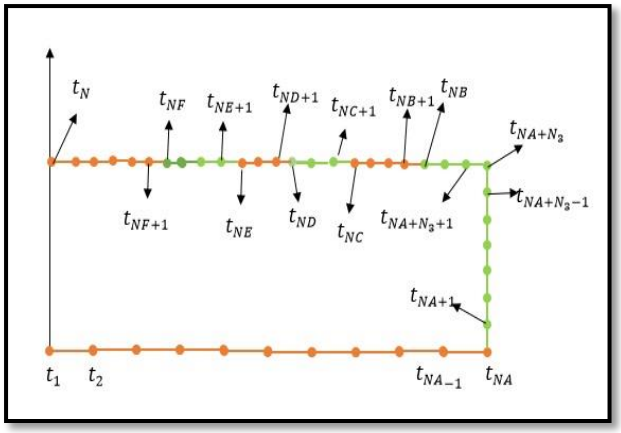

Figure (3): Equivalent for region V^d.

The microstrip antenna under test consists of a conductive material such as the patch, the ground plane, and two annular rings as well as the dielectric substrate between them. Because of these different surfaces, two types of boundary conditions must be satisfied. These conditions require vanishing of the tangential electric field component on the conductor surface, while the magnetic and electric fields continuity on the dielectric surface. The polarized currents within the dielectric surface and the current density on the conductor surface IE .Therefore the boundary condition equation for antenna can be described as follows [7, 8]:

Table (2): The distribution of basis function for internal equivalence region.

Basis function number	Location	Symbol	Equivalent symbol
$N_{15} = N_g - 1$	Ground plan	N_{15}	$N_A \equiv N_{15} + 1$
$N_{16} = N_3 + N_4$	Dielectric(N_{d1})	N_{d1}	$N_B \equiv N_A + N_{d1}$
$N_{17} = N_{p1} - 2$	External annular ring	N_{17}	$N_C \equiv N_B + N_{17} + 2$
$N_{18} = N_8$	Dielectric(N_{d2})	N_{d2}	$N_D \equiv N_C + N_{d2}$
$N_{19} = N_{P2} - 2$	Internal annular ring	N_{19}	$N_E \equiv N_D + N_{19} + 2$
$N_{20} = N_{12}$	Dielectric(N_{d3})	N_{d3}	$N_F \equiv N_E + N_{d3}$
$N_{21} = N_{P3} - 1$	Circular patch	N_{21}	$N \equiv N_F + N_{21} + 1$

$$\hat{n} \times \vec{E}^e = 0 on\ S_{ce} \dots (2a)$$
$$\hat{n} \times \vec{E}^d = 0 on\ S_{cd} \dots (2b)$$
$$\hat{n} \times \vec{E}^d = \hat{n} \times \vec{E}^e on\ S_{de} \dots (2c)$$
$$\hat{n} \times \vec{H}^d = \hat{n} \times \vec{H}^e on\ S_{de} \dots (2d)$$

Where $\hat{n}$ is the unit vector normal to the conductor and dielectric surface.

The surface equivalent electric and magnetic currents are:

$$\vec{J}_{ce} = \hat{n} \times \vec{H}^e on\ S_{ce} \dots (3a)$$
$$\vec{J}_{cd} = \hat{n} \times \vec{H}^d on\ S_{cd} \dots (3b)$$
$$\vec{J}_{de} = \hat{n} \times \vec{H}^e \quad on\ S_{de} \dots (3c)\vec{M}$$
$$= -\hat{n} \times \vec{E}^e on\ S_{de} \dots (3d)$$

The equivalent electric currents ($\vec{J}_{ce}, \vec{J}_{cd}, \vec{J}_{de}$) are generated on the conductor and dielectric surface where the equivalent magnetic currents $\vec{M}$ is generated on the dielectric surface only. Applying the equivalent principle on internal and external equivalent region of the problem yields the integral equations as follows:

On the generating curve of the surfaces $(S_{ce} + S_{de})$ for the external region:-

$$\hat{n} \times \vec{E}^e(\vec{J}_{ce} + \vec{J}_{de}, \vec{M}) = 0 \dots (4a)$$
$$\hat{n} \times \vec{H}^e(\vec{J}_{ce} + \vec{J}_{de}, \vec{M}) = 0 \dots (4b)$$

On the generating curve of the surfaces $(S_{cd} + S_{de})$ for the internal region:

$$\hat{n} \times \vec{E}^d\left(-\vec{J}_{cd} - \vec{J}_{de}, -\vec{M}\right) + \hat{n} \times \vec{E}^d(\vec{J}^{id}, 0) = 0 \dots (4c)$$
$$\hat{n} \times \vec{H}^d\left(-\vec{J}_{cd} - \vec{J}_{de}, -\vec{M}\right) + \hat{n} \times \vec{H}^d(\vec{J}^{id}, 0) = 0 \dots (4d)$$

Where $\vec{H}^a(\vec{J}, \vec{M})$ and $\vec{E}^a(\vec{J}, \vec{M})$ represent the magnetic and electric fields due to the currents $\vec{J}$ and $\vec{M}$, radiated in media characterized by (μ_a, ε_a) .The symbol (a) represents the radiation media characterized by (μ_e, ε_e) and (μ_d, ε_d) , while $\vec{H}^d(\vec{J}^{id},0)$ and $\vec{E}^d(\vec{J}^{id},0)$ represents the magnetic and electric fields due to the currents of the feed ($\vec{J}^{id}$) .

Reformulate equation (3) for the equivalent surfaces (S_{cd}, S_{ce}, S_{de}) gives:

$$(\vec{J}_{ce} + \vec{J}_{de}) = \sum_{n=-\infty}^{\infty} \left[\sum_{i=1}^{2(N-N_d-10)} I_{ni}^{1e} \bar{J}_{ni}^{1e} + \sum_{i=1}^{2(N_d-4)} I_{ni} \bar{J}_{ni}^{2e} \right] \dots\dots (5a)$$

$$(\vec{J}_{cd} + \vec{J}_{de}) = \sum_{n=-\infty}^{\infty} \left[\sum_{i=1}^{2(N-N_d-10)} I_{ni}^{1d} \bar{J}_{ni}^{1d} + \sum_{i=1}^{2(N_d-4)} I_{ni} \bar{J}_{ni}^{2d} \right] \dots\dots (5b)$$

$$\vec{M} = \eta_e \sum_{n=-\infty}^{\infty} \sum_{i=1}^{2(N_d-4)} K_{ni} \bar{M}_{ni} \dots\dots (5c)$$

Substitute equation (5) in to equation (4) and using a Galerkin's method which is one of the most appropriate calculation methods for the selection of the weight functions ($W = J^*$) to get [9].

$$\vec{W}(t,\varphi) = \vec{W}^t(t,\varphi) + \vec{W}^{\varphi}(t,\varphi) = \sum_{m=-\infty}^{\infty} \sum_{j=1}^{N-14} \left[\bar{W}_{mj}^t(t,\varphi) + \bar{W}_{mj}^{\varphi}(t,\varphi) \right] \dots\dots (6a)$$

$$\bar{W}_{mj}^{\alpha}(t,\varphi) = \hat{u}_{\alpha} f_j(t) e^{-jm\varphi} \quad \dots\dots (6b)$$

Where, $f_i(t) = \frac{T(t-t_i)}{\rho}$ …… (6c)

and

$$\sum_{j=1}^{2(N-N_d-10)}\left[\sum_{i=1}^{2(N-N_d-10)} I_{ni}^{1e}\langle\vec{W}_{nj}^{1e},\vec{E}_{tan}^{e}(\vec{J}_{ni}^{1e},0)\rangle + \sum_{i=1}^{2(N_d-4)} I_{ni}\langle\vec{W}_{nj}^{1e},\vec{E}_{tan}^{e}(\vec{J}_{ni}^{2e},0)\rangle + \eta_e \sum_{i=1}^{2(N_d-4)} K_{ni}\langle\vec{W}_{nj}^{1e},\vec{E}_{tan}^{e}(0,\vec{M}_{ni})\rangle\right] = 0 \quad on\ S_{ce} \ \dots\dots (7a)$$

$$\sum_{j=1}^{2(N-N_d-10)}\left[\sum_{i=1}^{2(N-N_d-10)} I_{ni}^{1d}\langle\vec{W}_{nj}^{1d},\vec{E}_{tan}^{d}(\vec{J}_{ni}^{1d},0)\rangle + \sum_{i=1}^{2(N_d-4)} I_{ni}\langle\vec{W}_{nj}^{1d},\vec{E}_{tan}^{d}(\vec{J}_{ni}^{2d},0)\rangle + \eta_e \sum_{i=1}^{2(N_d-4)} K_{ni}\langle\vec{W}_{nj}^{1d},\vec{E}_{tan}^{d}(0,\vec{M}_{ni})\rangle\right] = \langle\vec{W}_{nj}^{1d},\vec{E}_{tan}^{d}(\vec{J}^{id})\rangle \ on\ S_{cd} \quad \dots\dots (7b)$$

$$\sum_{j=1}^{2(N_d-4)}\left[\sum_{i=1}^{2(N-N_d-10)} \{I_{ni}^{1e}\langle\vec{W}_{nj}^{2e},\vec{E}_{tan}^{e}(\vec{J}_{ni}^{1e},0)\rangle + I_{ni}^{1d}\langle\vec{W}_{nj}^{2d},\vec{E}_{tan}^{d}(\vec{J}_{ni}^{1d},0)\rangle\} + \sum_{i=1}^{2(N_d-4)} \{\{I_{ni}\langle\vec{W}_{nj}^{2e},\vec{E}_{tan}^{e}(\vec{J}_{ni}^{2e},0)\rangle + I_{ni}\langle\vec{W}_{nj}^{2d},\vec{E}_{tan}^{d}(\vec{J}_{ni}^{2d},0)\rangle\}\} + \eta_e \sum_{i=1}^{2(N_d-4)} \{K_{ni}\langle\vec{W}_{nj}^{2e},\vec{E}_{tan}^{e}(0,\vec{M}_{ni})\rangle + K_{ni}\langle\vec{W}_{nj}^{2d},\vec{E}_{tan}^{d}(0,\vec{M}_{ni})\rangle\}\right] = \langle\vec{W}_{nj}^{2d},\vec{E}_{tan}^{d}(\vec{J}^{id})\rangle \ on\ S_{de} \quad \dots\dots (7c)$$

$$\sum_{j=1}^{2(N_d-4)}\left[\sum_{i=1}^{2(N-N_d-10)} \{I_{ni}^{1e}\langle\vec{W}_{nj}^{3},\vec{H}_{tan}^{e}(\vec{J}_{ni}^{1e},0)\rangle + I_{ni}^{1d}\langle\vec{W}_{nj}^{3},\vec{H}_{tan}^{d}(\vec{J}_{ni}^{1d},0)\rangle\} + \sum_{i=1}^{2(N_d-4)} \{\{I_{ni}\langle\vec{W}_{nj}^{3},\vec{H}_{tan}^{e}(\vec{J}_{ni}^{2e},0)\rangle + I_{ni}\langle\vec{W}_{nj}^{3},\vec{H}_{tan}^{d}(\vec{J}_{ni}^{2d},0)\rangle\}\} + \eta_e \sum_{i=1}^{2(N_d-4)} \{K_{ni}\langle\vec{W}_{nj}^{3},\vec{H}_{tan}^{e}(0,\vec{M}_{ni})\rangle + K_{ni}\langle\vec{W}_{nj}^{3},\vec{H}_{tan}^{d}(0,\vec{M}_{ni})\rangle\}\right] = \langle\vec{W}_{nj}^{3},\vec{H}_{tan}^{d}(\vec{J}^{id})\rangle \ on\ S_{de} \quad \dots\dots (7d)$$

Linear equations (7) can be written in the following matrix form:

$$[\vec{T}_{nm}][\vec{I}_n] = [\vec{V}_n] \ \dots\dots (8)$$

The impedance and admittance submatrices are represented in a square matrix $[\vec{T}_n]$, the unknown expansion coefficients of J and M are given in a column matrix $[\vec{I}_n]$. Also, the excitation matrix is in the form of a column matrix $[\vec{V}_n]$.

And can be written as:

$$[\vec{T}_n] = \begin{bmatrix} [Z_{ce,ce}^{1e}]_n & [0]_n & [Z_{ce,de}^{2e}]_n & \eta_e[Y_{ce,de}^{3e}]_n \\ [0]_n & [Z_{cd,cd}^{1d}]_n & [Z_{cd,de}^{2d}]_n & \eta_e[Y_{cd,de}^{3d}]_n \\ [Z_{de,ce}^{1e}]_n & [Z_{de,cd}^{1d}]_n & [Z_{de,de}^{2e}+Z_{de,de}^{2d}]_n & \eta_e[Y_{de,de}^{3e}+Y_{de,de}^{3d}]_n \\ [Y_{de,ce}^{1e}]_n & [Y_{de,cd}^{1d}]_n & [Y_{de,de}^{2e}+Y_{de,de}^{2d}]_n & \eta_e[Z_{de,de}^{3e}+Z_{de,de}^{3d}]_n \end{bmatrix} \ \dots\dots (9)$$

$$[\vec{I}_n] \equiv \begin{bmatrix} [I^{1e}]_n \\ [I^{1d}]_n \\ [I\ ]_n \\ [K\ ]_n \end{bmatrix} \quad \ldots\ldots(10)$$

and,

$$[\vec{V}_n] = = \begin{bmatrix} [0]_n \\ [V_{cd}^{d}]_n \\ [V_{de}^{d}]_n \\ [I_{de}^{d}]_n \end{bmatrix} \quad \ldots\ldots(11)$$

Where (Z^{1e} ,Y^{1e}) and (Z^{1d} , Y^{1d}) submatrices represent the calculation of impedance Z and admittance *Y* due to the electric (for *Z*) and magnetic (for *Y*) surface current densities on the surfaces S_{ce} (exterior media) and S_{cd} (interior media), respectively. Also, (Z^{2e} ,Y^{2e}) and (Z^{2d} , Y^{2d}) submatrices represent the calculation of impedance Z and admittance *Y* due to the electric (for *Z*) and magnetic (for *Y*) surface current densities on the surface S_{de} for exterior or interior media, respectively. While (Z^{3e} ,Y^{3e}) and (Z^{3d} , Y^{3d}) submatrices represent the calculation of impedance Z and admittance *Y* due to the electric (for *Y*) and magnetic (for *Z*) surface current densities on the surface S_{de} for exterior or interior media, respectively. The first and second pairs of supplements {*(ce,ce), (ce,de), (cd,cd)……*} refer to the field and source surfaces, respectively. The index n denotes the number of azimuthal mode, and V_{cd}^{d}, V_{de}^{d} and I_{de}^{d} are the excitation submatrices, due to the electric and magnetic field sources on the surfaces, S_{cd}, S_{de} from the interior region. As was mentioned previously in this chapter, I^{1e} , I^{1d} ,I and K are the unknown coefficients of the equivalent electric (on the S_{ce} , S_{cd} and S_{de} surfaces) and magnetic (on the S_{de} surface only) current densities, respectively.

The radiation fields are calculated at the far field region (E_θ, E_ϕ) from induced electric and magnetic currents flowing on the surface of the conductor and the dielectric of the antennas so [11]:

$$E_\theta = -\frac{j\omega\mu_e}{4\pi\ r_o} e^{-jK_e r_o} F_1(\theta_o, \phi_o) \quad \ldots\ldots(12a)$$

$$E_\phi = -\frac{j\omega\mu_e}{4\pi r_o} e^{-jK_e r_o} F_2(\theta_o, \phi_o) \ldots\ldots(12b)$$

Where $F_1(\theta_o, \phi_o)$ and $F_2(\theta_o, \phi_o)$ are the integrals that represent the measurement coefficients carried out over the external surface of the CMSAL2AR in this form:-

$$F_1(\theta_o, \phi_o) = \int_s \left(\bar{J}(\bar{r}') \cdot \hat{\theta} + \frac{1}{\eta_e} \bar{M}(\bar{r}') \cdot \hat{\phi} \right) e^{-jK_e \hat{r}_o \bullet \bar{r}'} ds \ldots\ldots(13a)$$

$$F_2(\theta_o, \phi_o) = \int_s \left(\bar{J}(\bar{r}') \cdot \hat{\phi} - \frac{1}{\eta_e} \bar{M}(\bar{r}') \cdot \hat{\theta} \right) e^{-jK_e \hat{r}_o \bullet \bar{r}'} ds \ldots\ldots(13b)$$

where S is the exterior surface of the antenna, $\hat{r}_\circ$ a unit vector directed from the origin to the field point, and $\hat{\theta}_\circ, \hat{\phi}_\circ$ are the transverse unit vector in the direction of increasing θ and ϕ, respectively.

Results and Discussion

The proposed design, which study the contribution of the adjacent mode, shown an increased whenever the interference between them and the main mode occurs. This contribution will be effecting positive or negatively on the antenna's coefficients. This contribution of the adjacent mode will be calculated here for the CMSAL2AR excited byTM_{11}-mode.

Figures (4a),(4b),and(4c) show the contribution of the adjacent modes TM_{21}, TM_{02} with the main mode $TM_{11}$for the ratio $R_{ab} = 5.5$, and different (ab/ab_1) , which has been in the range value of (-18 dB→ -22dB) for TM_{21} mode and non-significant for the TM_{02} mode as recorded in Table (3). The table shows

the contribution of the adjacent mode interference values with the main mode for different ratios (R_{ab}). The contribution of TM_{21} – mode was effected positively on the directive gain of the propose antenna specially for the values$ab/ab_1 = 3.5$.

Also Figures (5a),(5b),and(5c) represent the contribution of the same adjacent mode TM_{21}, TM_{02} for ratio $R_{ab} = 6.5$, and different (ab/ab_1) value, which has been in the range value of (-30dB → -38dB) . This is non-effective contribution on the antenna parameter, which mean that there is no interference of the adjacent mode with the dominant mode.

Also Table (4) shows the best value for the gain

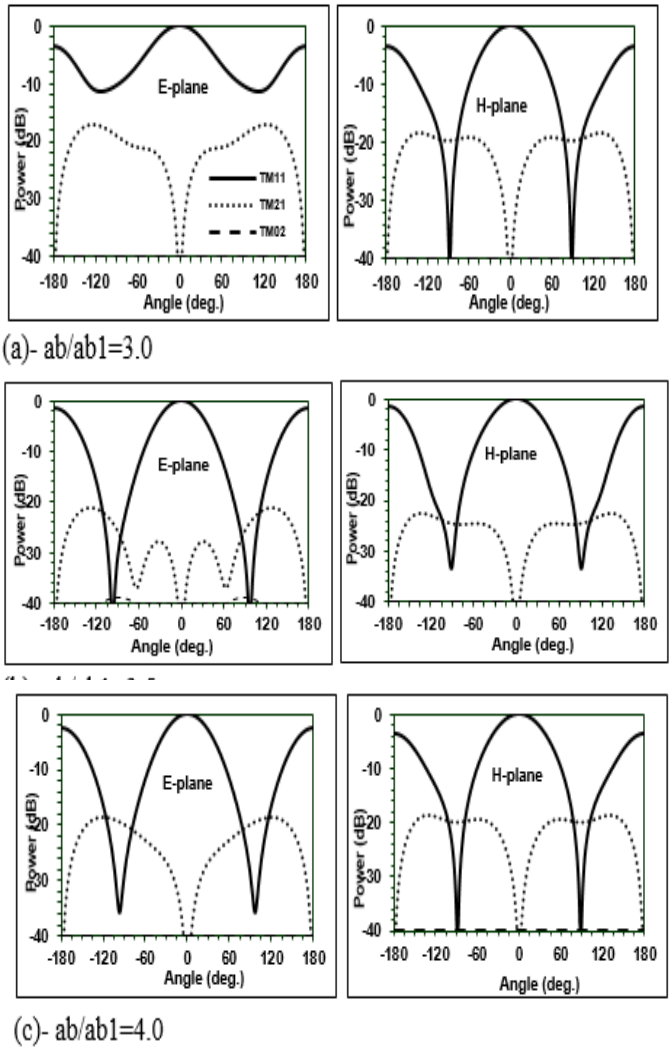

(a)- ab/ab1=3.0

(c)- ab/ab1=4.0

Figure (4): Contribution of the adjacent modes with the resonant mode TM11 of the CMSAL2AR for the ratio R_ab=5.5 ,and different (ab⁄([ab]_1)).

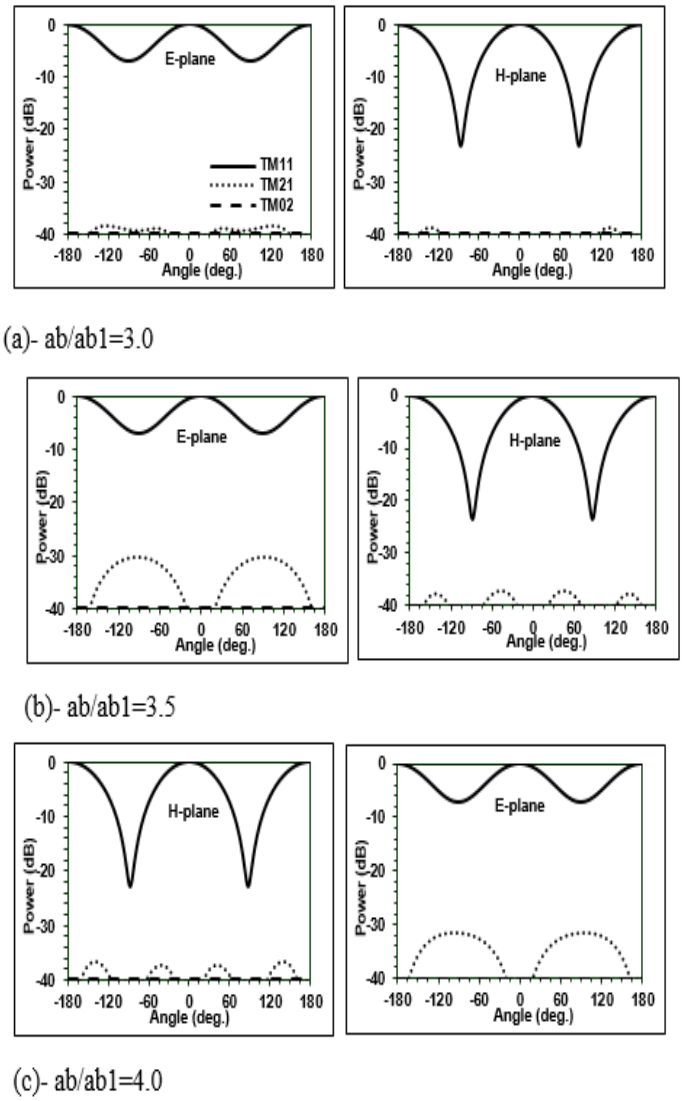

(a)- ab/ab1=3.0

(b)- ab/ab1=3.5

(c)- ab/ab1=4.0

Figure (5): Contribution of the adjacent modes with the resonant mode TM11 of the CMSAL2AR for the ratio R_ab=6.5 ,and different (ab⁄([ab]_1)).

$(G = 19.92\ dB)$ was obtained for the cient $(R_{ab} = 5.5)$, while the best value for the bandwidth $(BW = 19.9\%)$ was obtained for $(R_{ab} = 6.5)$.

Table (3): The contribution of adjacent modes interference with TM_{11} mode for different values of the ratio R_{ab} , and (ab/ab_1) .

R_{ab}	ab/ab1	Contribution mode E-plane		Contribution mode H-plane	
		TM_{21}	TM_{02}	TM_{21}	TM_{02}
5.5	3.0	-17	-----	-18	-----
	3.5	-21	-----	-22	-----
	4.0	-19	-----	-21	-----
5.6	3.0	-33	-----	-30	-----
	3.5	-30	-----	-34	-----
	4.0	-27	-----	-33	-----
5.7	3.0	-9	-----	-11	-----
	3.5	-20	-----	-22	-----
	4.0	-18	-----	-22	-----
5.8	3.0	-30	-----	-33	-----
	3.5	-26	-----	-22	-----
	4.0	-33	-----	-33	-----
5.9	3.0	-24	-----	-27	-----
	3.5	-26	-----	-22	-----
	4.0	-27	-----	-31	-----
6	3.0	-19	-----	-22	-----
	3.5	-22	-17	-26	-25
	4.0	-13	-15	-22	-22
6.1	3.0	-25	-----	-27	-----
	3.5	-27	-----	-30	-----
	4.0	-26	-----	-30	-----
6.2	3.0	-32	-----	-35	-----
	3.5	-31	-----	-35	-----
	4.0	-32	-----	-36	-----
6.3	3.0	-33	-----	-36	-----
	3.5	-32	-----	-37	-----
	4.0	-32	-----	-38	-----
6.4	3.0	-32	-----	-37	-----
	3.5	-31	-----	-38	-----
	4.0	-31	-----	-38	-----
6.5	3.0	-38	-----	-38	-----
	3.5	-30	-----	-37	-----
	4.0	-31	-----	-37	-----

Table (4): Radiation patterns parameter of CMSAL2AR excited by $TM_{11}-$ modefor different ratio of R_{ab} and(ab/ab_1).

Antenna Type	ab/ab1	$HP_H°$ (deg)	$HP_E°$ (deg)	Directive gain (dB)	BW% S=2
CMSAL2AR (R_{ab}=5.5)	3.0	72	68	17.52	13.58
	3.5	58	64	19.92	15
	4.0	60	66	19.36	11.13
CMSAL2AR (R_{ab}=5.6)	3.0	86	76	16.01	12.7
	3.5	84	76	16.21	17.26
	4.0	92	76	14.42	12.83
CMSAL2AR (R_{ab}=5.7)	3.0	64	66	18.8	11.6
	3.5	60	64	19.63	12.92
	4.0	64	66	18.8	13.86
CMSAL2AR (R_{ab}=5.8)	3.0	92	76	14.42	10.56
	3.5	88	76	14.81	11.79
	4.0	84	76	16.21	12.83
CMSAL2AR (R_{ab}=5.9)	3.0	84	76	15.21	12.64
	3.5	86	76	15.01	7.64
	4.0	84	76	15.21	7.16
CMSAL2AR (R_{ab}=6.0)	3.0	76	68	17.05	16.69
	3.5	74	68	17.28	9.811
	4.0	78	64	17.35	9.43
CMSAL2AR (R_{ab}=6.1)	3.0	84	76	15.21	11.32
	3.5	86	76	15.01	7.73
	4.0	84	76	15.21	7.54
CMSAL2AR (R_{ab}=6.2)	3.0	84	74	15.44	11.88
	3.5	80	64	17.13	11.32
	4.0	80	70	16.35	11.69
CMSAL2AR (R_{ab}=6.3)	3.0	88	80	14.36	11.88
	3.5	88	80	14.36	11.5
	4.0	88	80	14.36	11.13
CMSAL2AR (R_{ab}=6.4)	3.0	88	80	14.36	11.88
	3.5	88	80	14.36	16.60
	4.0	88	80	14.36	18.11
CMSAL2AR (R_{ab}=6.5)	3.0	88	80	14.36	12.07
	3.5	88	80	14.36	17.64
	4.0	88	80	14.36	19.9

Conclusions

In this paper CMSAL2AR is designed using the moment of method and simulation by using Fortran 90 language .The contribution of the adjacent mode was of positive effect at the ratio and .The bandwidths and directive gain increasing to (19.9%) and (19.92dB) respectively.

Reference

[1] Carver, K., and Mink, J., "Microstrip antenna technology" IEEE transactions on antennas and propagation 29.1 (1981): 2-24.

[2] Kumar, R., and Dhubkarya, D. D. "Design and analysis of circular ring microstrip antenna" Global Journal of Research In Engineering 11.1 (2011).

[3] Alexander, K., "Aperture-coupled microstrip patch antenna array", Diplomarbeit, Friedhofallee 4a/11, A-2232 Deutsch-Wagram, 1996.

[4] Nie, Z., Chew, W. C., & Lo, Y. T. "Analysis of the annular-ring-loaded circular-disk microstrip antenna." IEEE Transactions on Antennas and Propagation 38.6 (1990): 806-813.

[5] Bao, J., Wang, D., & Yung, E. K. N. (2007, June)." Radiation and scattering from bi-isotropic bodies of revolution." In Antennas and Propagation Society International Symposium, 2007 IEEE (pp. 5023-5026). IEEE.

[6] Dawod ,R. M ,"Concentric circular microstrip antenna novel design for enhancing the power bandwidth and the directive gain ",Ph. D. Thesis Submitted to the College of Science of Basrah University, Iraq, 2014.

[7] Durham, Timothy E., and Christos G. Christodoulou. "Integral equation analysis of dielectric aconducting bodies of revolution in the presence of arbitrary surfaces." IEEE transactions on antennas and propagation 43.7 (1995): 674-680.

[8]Rui, Xi, J. H., and Qing H. L. "Scattering from a composite body of revolution with fast inhomogeneous plane wave algorithm." Antennas and Propagation Society International Symposium (APSURSI), 978.1 2010: 4244-4968.

[9] Gupta, Dipali, and RajdeepShrivastava. "Triple Band Dual Circular Slot rectangular microstrip antenna" International Journal of computer applications 147.5(2016).

[10] Rachmansyah, Antonius Irianto, & A. Benny Mutiara, "Designing and manufacturing microstrip antenna for wireless communication at 2.4 GHz," International Journal of Computer and Electrical Engineering, 3. 5, October 2011.

[11] Alsager, A. F. "Design and analysis of microstrip patch antenna arrays." M.Sc. Thesis from University of College of Boras (2011).